SOL-GEL α -Al₂O₃ detectors: TL and OSL response to beta radiation beams

Ivón Oramas Polo*, Linda V.E. Caldas

Instituto de Pesquisas Energéticas e Nucleares/ Comissão Nacional de Energia Nuclear, IPEN/CNEN, Av. Prof. Lineu Prestes, 2242, 05508-000, São Paulo, SP, Brazil

ARTICLE INFO

Keywords:

SOL-GEL α -Al₂O₃ detector
beta radiation
TL
OSL

ABSTRACT

The dosimetric properties of the SOL-GEL α -Al₂O₃ detectors with several different concentrations of impurities were studied in beta radiation beams. For the characterization of the detectors, the TL and OSL techniques were used. A TL spectrum was acquired. The detectors showed adequate OSL and TL dosimetric characteristics, such as good reproducibility, a glow curve with the peak at ~ 230 °C at 5 °C/s of heating rate, adequate OSL decay curve, good linearity of response and high phosphor sensitivity. A thermal treatment study was also performed. Moreover, the calibration factors and the lower detection limits were determined for beta radiation. These characteristics indicate the suitability of SOL-GEL α -Al₂O₃ detectors for the establishment of a transfer system or alternative/complementary method for beta radiation dosimetry.

1. Introduction

The primary instrument established for the measurement of beta radiation is the extrapolation chamber (Böhm, 1986; Caldas, 1986). However, the calibration of dosimeters with this instrument must be performed under special laboratory conditions, with control of environmental conditions (temperature, humidity and pressure). In addition, the ionization chamber is heavy, its entrance window is very delicate, and the calibration procedures take a long time. The thermoluminescence (TL) and optically stimulated luminescence (OSL) techniques constitute alternative methods for beta radiation measurements.

The TL and OSL dosimeter responses to beta radiation beams have been studied by several authors (Caldas, 1986; Cross, 1997; Akselrod et al., 1999; Mancosu et al., 2005; Pinto et al., 2008; Yukihiro and McKeever, 2008; Nascimento et al., 2013; Kumar et al., 2013; Kumar et al., 2016). The material choice of the dosimeter is very important, because beta radiation is a weakly penetrating radiation.

Thin thermoluminescent (TL) dosimeters of materials with low atomic number, such as LiF, Li₂B₄O₃, Mg₂B₄O₇, Al₂O₃, among other materials, can be used for the calibration of beta radiation beams (ICRU, 1997). Some types of thin detectors have been prepared with TL high-sensitivity phosphors such as Mg₂B₄O₇:Dy, CaSO₄:Dy, Al₂O₃:C e LiF:Mg,Cu,P. The high sensitivity of the phosphor is very important, because the required surface density results in a very small amount of luminescent material (Akselrod et al., 1999).

Al₂O₃:C is the most studied and applied material for OSL, due to its high sensitivity. The OSL technique with Al₂O₃:C has the advantage

over TL, that when using light as a stimulus, it avoids the possible phenomenon of thermal quenching of the main luminescent centers (F-centers) at high heating rates (Akselrod et al., 1998; Yukihiro and McKeever, 2011). Another problem with this material is the high sensitivity of the TL signal to light exposure (Akselrod et al., 1990). In the OSL technique by controlling the power and the time of the stimulus in the OSL reader, a wide range of flexibility in use can be achieved. For example, if the LED power is increased and the stimulation time is reduced, a very fast signal reading is obtained (McKeever and Moscovitch, 2003; Villani et al., 2017). However, the Al₂O₃:C material is sensitive to visible light which may cause loss of signal due to light induced fading (Akselrod et al., 1990), as well as light induced OSL signal (light induced TL signal). This characteristic of the OSL technique could influence the measurements with possible errors due to accidental or intentional exposure to light. Therefore, the measurements require strict dark conditions room (McKeever and Moscovitch, 2003).

Göksu et al. (1999) have shown that thin-layer α -Al₂O₃:C dosimeters can be used successfully for the measurement of annual beta doses for retrospective dosimetry, and also for dating purposes. The response of Al₂O₃:C to standard beta radiation sources has been object of several studies (Akselrod et al., 1999; Pinto et al., 2008; Yukihiro and McKeever, 2008; Yukihiro and McKeever, 2011; Nascimento et al., 2013).

The sol-gel process is used to synthesize glasses and crystals by a colloidal route with an intermediate stage that includes a sol and/or a gel state. Through this process, it is possible to produce hybrid materials that do not exist naturally, and very pure and homogeneity products can be obtained by purifying the precursors (Pierre, 1998). The

* Corresponding author.

E-mail addresses: ivonoramas67@gmail.com (I.O. Polo), lcaldas@ipen.br (L.V.E. Caldas).

sol-gel process can be implemented in a usual infrastructure laboratory for the synthesis of luminescent materials because it is a relatively inexpensive method (Rivera, 2011). Neodymium doped and undoped aluminum oxide samples have been synthesized and produced by the sol-gel and by Pechini methods for dosimetric purposes. It was possible to find out that when materials are produced by different methods, they have different physical and dosimetric characteristics. The TL curves obtained by these methods are shown and analyzed (Bitencourt et al., 2010). Ferreira and Santos (2014) reported on the preparation and characterization of SOL-GEL α -Al₂O₃ detectors. For the production of sol-gel detectors, aluminum nitrate dissolved in alcohol was used. The following metals in the form of nitrates were added as dopants to this solution: Fe, Mg, Ca, Cr, Ni and Mo, as well as C. These impurities were added to some samples in their preparation in order to improve the sensitivity of these detectors, and they showed a TL sensitivity three times higher than that in samples without these impurities. The fabrication process, the temperature of the thermal treatment, the calcination time, the heating rates, etc., influence the physicochemical properties of the doped materials. Tatum et al. (2012) showed that calcinated α -Al₂O₃ samples above 1100 °C exhibited large TL and OSL signals. The SOL-GEL α -Al₂O₃ detectors were calcinated in a muffle furnace at 1200 °C (Ferreira and Santos, 2014). The detectors were irradiated and calibrated in a standard ¹³⁷Cs beam, and they were characterized using the TL technique.

The SOL-GEL α -Al₂O₃ detectors are of low cost, and they were produced in a usual laboratory without having to use techniques that are applied in laboratories for commercial purposes (for example the α -Al₂O₃:C material). Due to the sensitivity of these detectors, they are a good choice for beta radiation dosimetry. A study of TL and OSL dosimetric properties of the aluminum oxide synthesized with the sol-gel method with several different concentrations of impurities in BSS2 beta radiation beams has not been published yet.

The objective of the present work was to study the dosimetric properties of the SOL-GEL α -Al₂O₃ detectors in beta radiation beams for the establishment of a transfer system or alternative/ complementary method for beta radiation dosimetry. For the characterization of these detectors, the TL and OSL techniques were used. The material was characterized in terms of: thermal treatment study; reproducibility of response; relative intrinsic sensitivity factor; characterization of TL/OSL reader collimators; dose-response curves; calibration factors; lower detection limit; energy dependence; phosphor sensitivity and heating rate dependence.

2. Materials and methods

The Beta Secondary Standard BSS2 of the Calibration Laboratory (LCI) of IPEN was used. The main characteristics of the BSS2 sources are shown in Table 1.

The dosimetric system consists of the detectors, the TL/OSL reader, the thermal treatment system, and auxiliary materials that allow the dosimetric procedures.

The SOL-GEL α -Al₂O₃ detectors used in this work (named here as α -Al₂O₃ detectors), were produced by the sol-gel process using Aluminum Nitrate dissolved in alcohol as alumina precursor at the Dosimeter

Table 1
Main characteristics of the BSS2 beta sources (BSS2, 2005).

Characteristic	Radionuclide		
	¹⁴⁷ Pm	⁸⁵ Kr	⁹⁰ Sr/ ⁹⁰ Y
Nominal activity	3.7 GBq	3.7 GBq	460 MBq
Mean beta energy (MeV)	0.06	0.24	0.8
Calibration distance (cm)	20	30	11
Calibration date	19/11/2004	30/11/2004	19/11/2004
Approximate half-life (days)	958	3915	10,483

Calibration Laboratory of the Centro de Desenvolvimento da Tecnologia Nuclear/Comissão Nacional de Energia Nuclear (CDTN/CNEN) by Ferreira and Santos (2014). The metal nitrates used as dopants were: Fe, Mg, Ca, Cr, Ni and Mo, and urea as a carbon source. According to the producer, these detectors have the following dosimetric characteristics: high sensitivity, coefficient of variation between 2.1% and 3.8% for 15 irradiations, good linearity of response and good reproducibility (Ferreira and Santos, 2014).

The α -Al₂O₃ detectors present: (4.59 ± 0.01) mm diameter; (1.119 ± 0.010) mm thickness; and (51.8 ± 0.4) mg mass.

For TL and OSL measurements, the RISØ TL/OSL-DA20 system was used. The system allows up to 48 samples to be individually heated up to 700 °C. The measurements are performed in a vacuum chamber. The emitted luminescence is measured by a light detection system composed of a photomultiplier and suitable detection filters (DTU Nutech, 2015).

The detectors were irradiated using a RISØ ⁹⁰Sr/⁹⁰Y beta source with 0.5 Gy for the thermal treatment study, reproducibility of response test, characterization of TL/OSL reader collimators, OSL and TL response, and heating rate dependence study. Also, the detectors were irradiated in the BSS2 beta radiation beams with different doses for the dose-response curves, the determination of the calibration factors, the lower detection limit (LDL) determination, the phosphor sensitivity and the energy dependence studies. The measurements were taken in a dark room to avoid the influence of light on the response. For all TL measurements, the heating rate was 5 °C/s and the maximum temperature was 350 °C. The TL measurements were performed in a N₂ atmosphere. The emission from the samples was detected by a photomultiplier tube after passing through the Hoya U-340 UV filter with 7.5 mm thickness and 45 mm diameter (transmission band 250–390 nm FWHM). For OSL measurements, the constant light intensity (CW-OSL) mode was provided by 470 nm blue LEDs with a 60 s counting and 90% of power.

In addition to all components of the RISØ TL/OSL-DA20 system, there are four collimators (diameter of 20 mm) in LCI/IPEN whose function is to increase or decrease the intensity of the luminescent signal. The internal holes of the black cardboard paper collimators are approximately: 1.9 mm; 2.5 mm; 5.8 mm and 10 mm (Collimators 1, 2, 3 and 4). It has been shown that for certain absorbed dose values, the photomultiplier reader reached the limit established for its operation. Therefore, a study for signal collimators response was necessary. To determine the collimator correction factors, Eq. (1) was used:

$$F_{col} = \bar{M}_0 / \bar{M}_{col} \quad (1)$$

where \bar{M}_0 is the mean value of the dosimeter response without the use of collimator, and \bar{M}_{col} is the mean value of the dosimeter response with the use of collimator.

The study was performed without collimators and after using the four collimators for both TL and OSL techniques.

For the measurement of the TL spectrum, the Ocean Optics QE65 Pro Spectrometer was used. This spectrometer has a detector with 1044 × 64 element CCD array from Hamamatsu and its spectral range is 200 up to 1100 nm with window (QE65 Pro, 2018). The optical fiber used was a UV-vis solarization-resistant fiber, with 1.0 mm core diameter, and it presents a relative transmission better than 80% in the range of 250 – 900 nm.

The thermal treatment was carried out in a Provecto Analytica furnace, model MFLO1000. The characteristics of this furnace are the following: heating provided by a microwave system, heating rate of 0.95 °C/s, and maximum temperature of (1000 ± 3) °C. This was the treatment chosen for the detectors, because both OSL and TL techniques were utilized.

In Fig. 1 the irradiation holder of the dosimeters and the holder for carrying out the annealing treatment are shown. The holder material for the irradiation is polymethyl methacrylate (PMMA), with the following dimensions: 110 mm × 110 mm × 18 mm. This holder allows the simultaneous irradiation of 25 dosimeters, and the holder cover is a

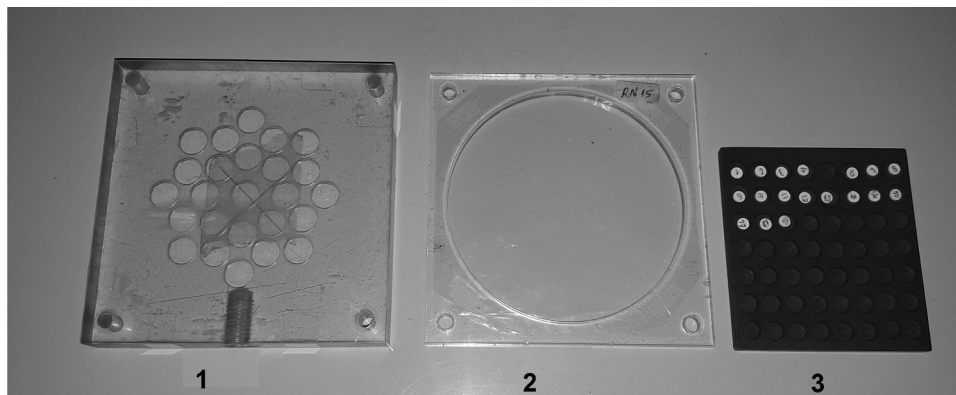


Fig. 1. Holders for: irradiation of the dosimeters (1 and 2) and for carrying out the thermal treatment (3).

polyester film sheet (Hostaphan) of 0.015 mm. The material of the annealing holder is copper, and it has the following dimensions: 75 mm × 80 mm × 8 mm. This holder allows the placement of 56 dosimeters.

The determination of the dosimetric system calibration factor was carried out in two different ways. The first method consisted in averaging all the individual factors for absorbed doses, and the second one consisted in a linear fitting of the calibration curve (Furetta, 2008).

The lower detection limit was determined taking three times the standard deviation of the zero dose reading (Furetta, 2008; Furetta and Weng, 1998).

3. Results and discussion

The results of the tests and studies carried out are presented in this section.

3.1. TL spectrum

Fig. 2 shows the TL spectrum as a function of temperature and wavelength, recorded at 5 K/s by a spectrometer and an optical fiber. A sample was irradiated at 10 Gy using the RISØ TL/OSL-DA20 $^{90}\text{Sr}/^{90}\text{Y}$ source. The spectrum revealed peaks at around 420 nm, 700 nm, 750 nm and 800 nm. The dosimetric peak of SOL-GEL $\alpha\text{-Al}_2\text{O}_3$ is at around 508 K (235 °C) and 420 nm. This band coincides with emission

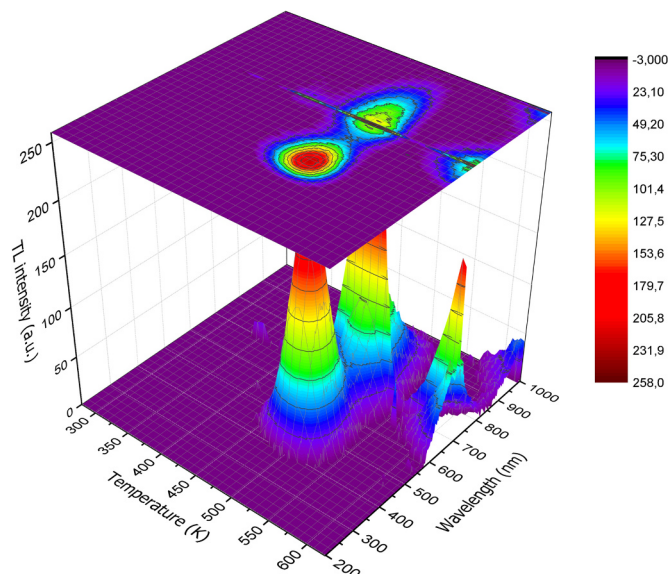


Fig. 2. TL emission spectrum of a $\alpha\text{-Al}_2\text{O}_3$ detector irradiated with 10 Gy using the RISØ TL/OSL-DA20 ($^{90}\text{Sr}/^{90}\text{Y}$).

bands in F center (oxygen vacancies with two electron captures) (Yukihara et al., 2003; Akselrod et al., 2006). The infrared emission (IR) centered near 700 nm is probably attributed to the presence of Fe^{3+} as impurity in the crystal lattice (Valle et al., 2004). Some authors associated the emission at 750 nm to the F_2^+ (2Mg) centers (Akselrod and Akselrod, 2006; Rodriguez et al., 2011; Kalita and Chithambo, 2017). The strong emission in the 800 nm band could also be associated with the presence of Fe^{3+} in the crystal (Rotman et al., 1989; Varney et al., 2011).

3.2. Thermal treatment study

Nineteen detectors were irradiated with a dose of 0.5 Gy of the RISØ TL/OSL-DA20 $^{90}\text{Sr}/^{90}\text{Y}$ source. The combination of time and annealing temperature were selected from the data reported in the literature for $\alpha\text{-Al}_2\text{O}_3\text{:C}$ and $\text{Al}_2\text{O}_3\text{:Cr}$ materials; for these materials 1 h at 400 °C and 15 min at 350 °C are recommended, respectively (Furetta, 2008). Initially, the detectors were annealed at the temperature of 400 °C during 30 min. Thereafter, the temperature was raised to 450 °C, 500 °C, 600 °C and 650 °C, maintaining the time of 30 min. After each thermal treatment, the intrinsic background was obtained, and the average response was determined.

Table 2 shows the values obtained for the thermal treatment study for $\alpha\text{-Al}_2\text{O}_3$ samples.

It can be observed that for the temperature of 600 °C, the S.D. and the C.V. presented lower values than for other temperatures. Therefore, the thermal treatment of 600 °C during 30 min was chosen for reutilization of these detectors.

3.3. Reproducibility of response

For this test, nineteen detectors were used. They were irradiated with identical doses as for the thermal treatment study. Afterwards, a TL reading, the thermal treatment and a reading of background signal were carried out. This procedure was repeated for 10 cycles.

The analysis of the mean and S.D. values identified the different sources of variation in the system reproducibility. The C.V. of each detector was calculated. Ten detectors were chosen as a batch, because they presented C.V. values lower than 10%. The total batch reproducibility was essentially due to the individual reproducibility of each

Table 2

Thermal treatment study for $\alpha\text{-Al}_2\text{O}_3$ detectors (S.D.: Standard deviation of TL values; C.V.: Coefficient of variation).

Temperature (°C)	400	450	500	600	650
Residual TL (background) (a.u.)	3191	2998	2944	2931	3000
S.D. (a.u.)	87	69	98	62	69
C.V. (%)	2.7	2.3	3.3	2.1	2.3

Table 3
Relative intrinsic sensitivity factors for each detector group.

Detector number	Relative intrinsic sensitivity factor for OSL	Detector number	Relative intrinsic sensitivity factor for TL
1	0.91 ± 0.05	11	0.90 ± 0.04
2	0.72 ± 0.04	12	0.80 ± 0.05
8	1.36 ± 0.08	16	1.87 ± 0.11
9	0.91 ± 0.07	18	0.87 ± 0.05
10	1.49 ± 0.06	19	1.05 ± 0.09

detector. Therefore, a relative intrinsic sensitivity factor (or individual correction factor) for each of them was utilized.

3.4. Relative intrinsic sensitivity factor

Due to the individual sensitivity of each dosimeter, it was necessary to determine their correction factors. The intrinsic sensitivity factor was determined by the procedure recommended by Furetta (Furetta, 2008).

The batch was divided into 2 groups of 5 detectors. The first group was chosen for the OSL technique, and the second one, for the TL technique. Table 3 shows the values of the relative intrinsic sensitivity factor for each detector group.

The correction factors lead to the reduction of the uncertainties of the net readings. The use of the correction factors allowed achieving a better reproducibility of the response of the system.

3.5. Characterization of TL/OSL reader collimators

The α-Al₂O₃ detectors exhibit high sensitivity to radiation. For the dose-response curve determination, a dose range of the radiation sources should be established. It has been shown that for certain absorbed doses, the photomultiplier reader reaches the limit established for its operation. Therefore, a study of the response variation with different collimators was necessary.

This study was performed without any collimator, and with the four collimators for both TL and OSL techniques. A dose of 0.5 Gy at the RISØ TL/OSL-DA20 (⁹⁰Sr/⁹⁰Y) was established. From the values of the integral of the response curves when using the collimators, and without using them, the correction factors were determined for all of the collimators (Table 4).

3.6. OSL and TL response of the α-Al₂O₃ detectors

Figs. 3 and 4 show the OSL decay curves and the glow curves of the α-Al₂O₃ detectors. The glow curves for the three beta sources presented the dosimetric peak at approximately 230 °C. Akselrod et al. (1996) reported on a dosimetric peak at about 190 °C for a thin powder layer of Al₂O₃:C detectors for a 5 °C/s heating rate. The material producer reported for these detectors a dosimetric peak at 198 °C in gamma beams of ¹³⁷Cs for a 2 °C/s heating rate (Ferreira and Santos, 2014), but the dosimetric characteristics of this material may differ from one laboratory to another, and they depend on the reading conditions.

Table 4
Correction factors for the collimators.

Collimator	Correction factor	
	OSL	TL
Without	1	1
1	739.1 ± 56.4	493.0 ± 74.1
2	169.0 ± 10.9	117.3 ± 10.9
3	29.99 ± 2.04	29.3 ± 2.4
4	9.5 ± 0.5	9.5 ± 0.7

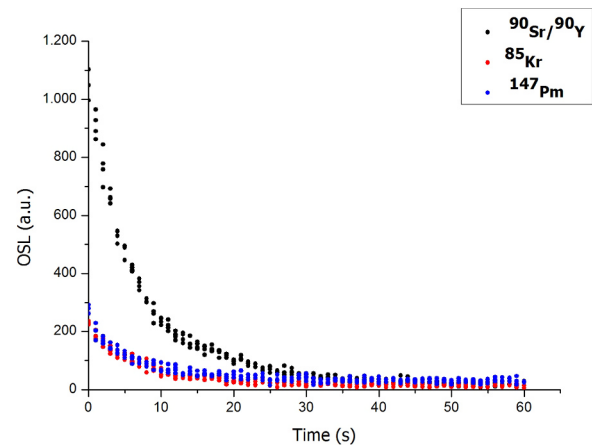


Fig. 3. Optically stimulated luminescence (OSL) decay curves of α-Al₂O₃ detectors in BSS2 beta radiation beams.

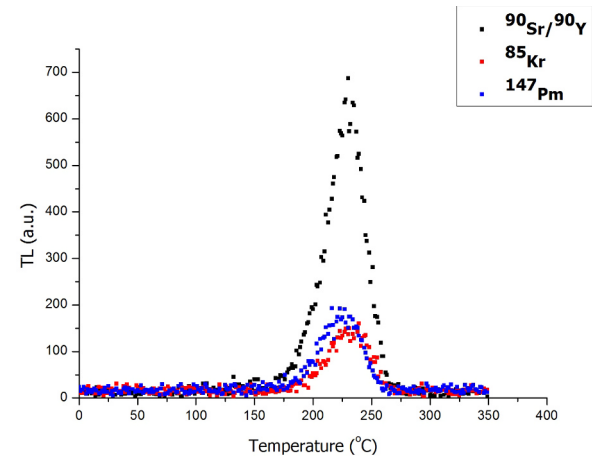


Fig. 4. Thermoluminescence (TL) glow curves of α-Al₂O₃ detectors in BSS2 beta radiation beams. The maximum emission was observed at 230 °C (heating rate of 5 °C/s).

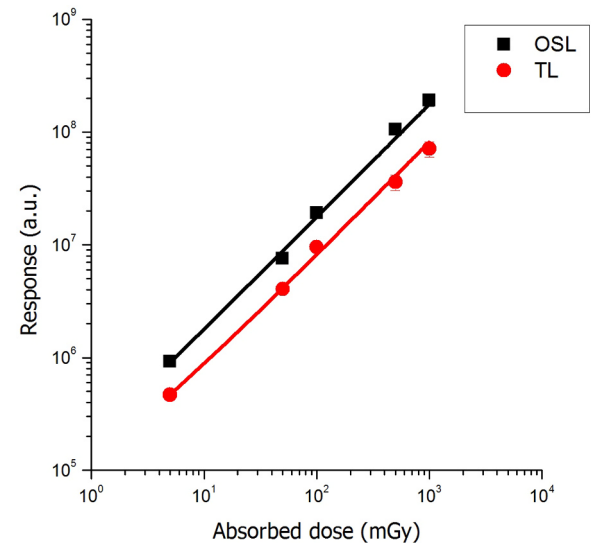


Fig. 5. Detectors of α-Al₂O₃, OSL and TL dose-response to ⁹⁰Sr/⁹⁰Y beta radiation beam.

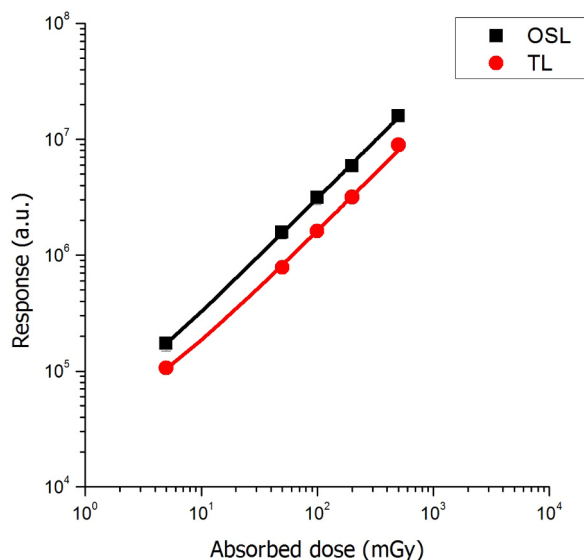


Fig. 6. Detectors of $\alpha\text{-Al}_2\text{O}_3$, OSL and TL dose-response to ^{85}Kr beta radiation beam.

3.7. Dose-response curves

The OSL and TL dose-response curves of $^{90}\text{Sr}/^{90}\text{Y}$, ^{85}Kr and ^{147}Pm sources are shown in Figs. 5, 6 and 7, respectively. For the $^{90}\text{Sr}/^{90}\text{Y}$ source, the dose range was 5 mGy to 1 Gy; for the ^{85}Kr source, the range was 5–500 mGy, and for the ^{147}Pm source, the range was 5–30 mGy. The OSL and TL dose responses were obtained by plotting the OSL and TL intensity versus dose, and the data was fitted to a straight line using a standard linear regression. For the $^{90}\text{Sr}/^{90}\text{Y}$ source, the coefficient of determination (R^2) of the linear regression was 0.97223 for OSL and 0.97982 for TL. For the ^{85}Kr source, R^2 was 0.99881 for OSL and 0.99572 for TL. For the ^{147}Pm source, R^2 was 0.99015 for OSL and 0.8895 for TL. It can be considered that the responses present linearity over the investigated dose ranges. In the case of the ^{147}Pm source, the uncertainties were large, and the TL dose-response curve showed the R^2 coefficient different from unity due to the attenuation in the air that is characteristic of this source. In addition, at the time of the study this source had an activity of only 0.13 GBq.

Akselrod et al. (1996) reported on linearity in the TL dose range from 10 μGy to 15 Gy for the $^{90}\text{Sr}/^{90}\text{Y}$ beta source. Pinto et al. (2008)

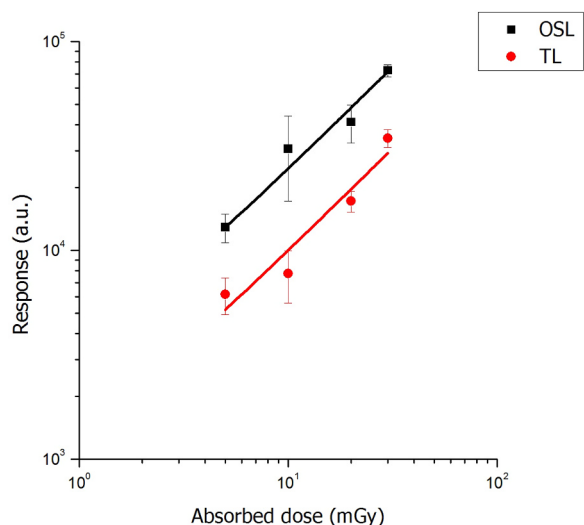


Fig. 7. Detectors of $\alpha\text{-Al}_2\text{O}_3$, OSL and TL dose-response to ^{147}Pm beta radiation beam.

Table 5
Calibration factors for $\alpha\text{-Al}_2\text{O}_3$ detectors.

Source	OSL calibration factor (mGy/u.a.)		
	Calculation	Linear fitting	Difference (%)
$^{90}\text{Sr}/^{90}\text{Y}$	$(5.5 \pm 0.4) \times 10^{-6}$	$(5.70 \pm 0.26) \times 10^{-6}$	3.5
^{85}Kr	$(3.18 \pm 0.08) \times 10^{-5}$	$(3.26 \pm 0.19) \times 10^{-6}$	2.5
^{147}Pm	$(4.03 \pm 0.33) \times 10^{-4}$	$(4.2 \pm 0.4) \times 10^{-4}$	4.0
	TL calibration factor (mGy/u.a.)		
$^{90}\text{Sr}/^{90}\text{Y}$	$(1.23 \pm 0.08) \times 10^{-5}$	$(1.24 \pm 0.06) \times 10^{-5}$	0.8
^{85}Kr	$(5.9 \pm 0.3) \times 10^{-5}$	$(6.2 \pm 0.3) \times 10^{-5}$	4.8
^{147}Pm	$(1.03 \pm 0.11) \times 10^{-3}$	$(1.04 \pm 0.12) \times 10^{-3}$	1.0

reported on linearity in the OSL dose range from 0.1 mGy to 10 mGy for the $^{90}\text{Sr}/^{90}\text{Y}$ beta source.

Table 5 shows the OSL and TL calibration factors for $\alpha\text{-Al}_2\text{O}_3$ detectors. The calibration factors were obtained by linear fitting, and by calculating the mean values of the absorbed dose individual factors. The calibration factors obtained in both cases are within the range of uncertainties. The differences were smaller than 5%.

3.8. Lower detection limit

The lower detection limit (LDL) was determined for the OSL and TL techniques for each source. The results are shown in Table 6.

The values in Table 6 show that the $\alpha\text{-Al}_2\text{O}_3$ detectors present a lower LDL for the OSL response than for the TL response. The results obtained show that these detectors are suitable for the measurement of very low doses. Akselrod et al. (1996) detected TL doses as small as 10 μGy for the $^{90}\text{Sr}/^{90}\text{Y}$ beta source.

3.9. Energy dependence

The $\alpha\text{-Al}_2\text{O}_3$ detectors were exposed to 5 mGy of the BSS2 beta radiation sources. The $^{90}\text{Sr}/^{90}\text{Y}$ source was considered as a reference, and the results of OSL and TL response were normalized to the energy from this source. Fig. 8 shows the variation of the OSL and TL responses as a function of the beam energy. The response was normalized to the $^{90}\text{Sr}/^{90}\text{Y}$ source intensity.

A strong energy dependence of these detectors to the BSS2 beta radiation system can be observed. The results are similar to those obtained by Akselrod et al. (1996), Akselrod et al. (1999) and Pinto et al. (2008) for $\text{Al}_2\text{O}_3\text{:C}$ detectors. The material producer reported also an energy dependence of the SOL-GEL $\alpha\text{-Al}_2\text{O}_3$ detectors in photon beams from 33 keV to 662 keV (Ferreira and Santos, 2014).

3.10. Phosphor sensitivity

The sensitivity of a phosphor is expressed by:

$$s = I/(D*m) \tag{2}$$

where I is the OSL or TL emission; D is the given dose in the linear region of the calibration curve, and m is the phosphor mass (Furetta, 2008).

The dose of 50 mGy was chosen for the cases of $^{90}\text{Sr}/^{90}\text{Y}$ and ^{85}Kr sources, and 10 mGy for ^{147}Pm source. Table 7 shows the intrinsic

Table 6
Lower detection limits, as function of the beam energy.

Source	Energy (MeV)	LDL (μGy)	
		OSL	TL
$^{90}\text{Sr}/^{90}\text{Y}$	0.80	5.40 ± 0.20	11.2 ± 0.6
^{85}Kr	0.24	22.8 ± 1.3	47.7 ± 2.5
^{147}Pm	0.06	624.2 ± 53.4	1406.03 ± 167.08

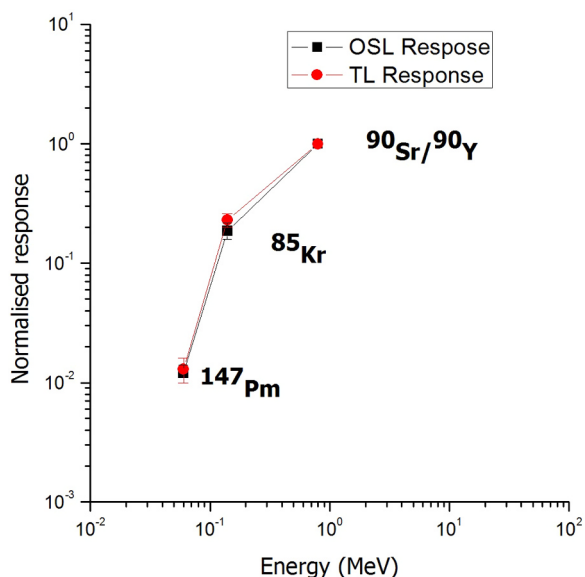


Fig. 8. Energy dependence of OSL and TL response of α -Al₂O₃ detectors to beta radiation.

Table 7

Intrinsic sensitivity of the α -Al₂O₃ detectors for the OSL and TL responses of $^{90}\text{Sr}/^{90}\text{Y}$, ^{85}Kr and ^{147}Pm sources.

Sensitivity (Counts/mGy.g)		
$^{90}\text{Sr}/^{90}\text{Y}$	^{85}Kr	^{147}Pm
OSL		
$(2.9 \pm 0.8) \times 10^6$	$(6.04 \pm 0.24) \times 10^5$	$(5.8 \pm 0.6) \times 10^4$
TL		
$(2.5 \pm 0.9) \times 10^6$	$(5.30 \pm 0.26) \times 10^5$	$(5.1 \pm 0.6) \times 10^4$

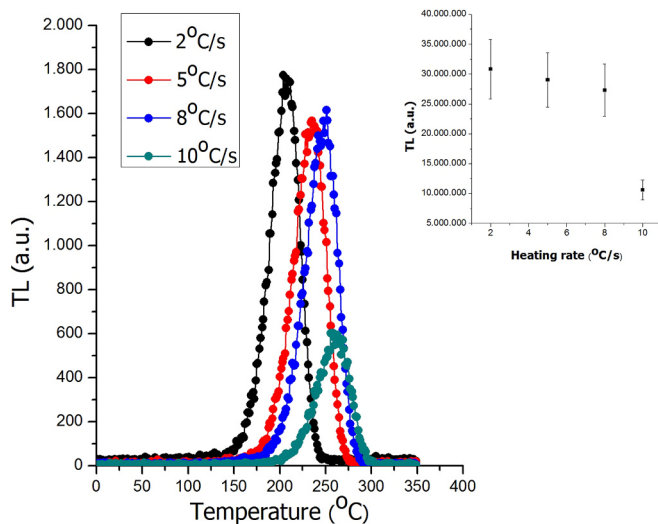


Fig. 9. Glow curves of α -Al₂O₃ samples at different heating rates and variation of the α -Al₂O₃ detectors TL response as a function of the readout heating rate of the RISØ TL/OSL-DA20 ($^{90}\text{Sr}/^{90}\text{Y}$).

phosphor sensitivity values for the OSL and TL responses of each source.

From these results, it can be observed that the material α -Al₂O₃ has a high intrinsic sensitivity to beta radiation. The sensitivity of the OSL response is greater than that of the TL response.

3.11. Heating rate dependence

For the study of the heating rate dependence in the readout, the detectors were exposed to the $^{90}\text{Sr}/^{90}\text{Y}$ reader source radiation beam. The reader was configured for a heating rate of 2 °C/s to 10 °C/s. Fig. 9 shows the glow curves of detector 8 that was chosen arbitrarily for the visualization purposes. The detector showed a decrease in TL response as the heating rate was increased. As the heating rate increased, the peak temperature shifted, and its intensity was reduced. Fig. 9 shows also the α -Al₂O₃ detector TL response as a function of the variation of the readout heating rate. By increasing the heating rate, a considerable increase of the crystal surface electrons is produced. According to the literature, the materials present different responses when the heating rate in the reader is varied. Alumina shows a TL signal loss as the heating rate increases (McKeever et al., 1995; Akserlod et al., 1998; Kitis, 2002; Pagonis et al., 2011; Kalita and Chithambo, 2017). This behavior suggests that the α -Al₂O₃ detectors are susceptible to thermal quenching, but it remains as a subject for further research.

4. Conclusions

The dosimetric properties of the α -Al₂O₃ detectors were investigated in standard beta radiation beams. A study of thermal treatments was carried out. The TL spectrum recorded at 5 K/s after beta irradiation to 10 Gy revealed peaks at approximately 420 nm, 700 nm, 750 nm and 800 nm. The detectors showed suitable OSL and TL dosimetric characteristics, such as good reproducibility, a glow curve with a 230 °C TL peak, adequate OSL decay curve, good linearity of response and high phosphor sensitivity. The detectors are appropriate for the measurement of very low doses. These characteristics indicate the suitability of α -Al₂O₃ for the establishment of a transfer system or an alternative/complementary method for beta radiation dosimetry. Future investigations are necessary for the study of the heating rate dependence and the phenomenon of thermal quenching.

Acknowledgments

The α -Al₂O₃ detectors were gently offered by Dr. Hudson Ferreira from the Centro de Desenvolvimento da Tecnologia Nuclear (CDTN/CNEN), Brazil, to whom the authors are very grateful. The authors thank also the partial financial support of the Brazilian funding agencies Conselho Nacional de Desenvolvimento Científico e Tecnológico (Project: 142297/2015-1, fellowship of I.O. Polo, and 301335/2016-8), Fundação de Amparo à Pesquisa do Estado de São Paulo (Project: 2008/57863-2) and Ministério da Ciência, Tecnologia, Inovações e Comunicação INCT Project: Radiation Metrology in Medicine (Project: 573659/2008-7).

References

- Akserlod, A., Akserlod, M.S., Agersnap Larsen, N., Banerjee, D., Botter-Jensen, L., Christensen, P., Lucas, A.C., McKeever, S.W.S., Yoder, R.C., 1999. Optically stimulated luminescence response of Al₂O₃ to beta radiation. *Radiat. Prot. Dosim.* 85 (1–4), 125–128.
- Akserlod, M.S., Akserlod, A.E., 2006. New Al₂O₃:C,Mg crystals for radiophotoluminescent dosimetry and optical imaging. *Radiat. Prot. Dosim.* 119 (1–4), 218–221.
- Akserlod, M.S., Botter-Jensen, L., McKeever, S.W.S., 2006. Optically stimulated luminescence and its use in medical dosimetry. *Radiat. Meas.* 41 (1), S78–S99.
- Akserlod, M.S., Kortov, V.S., Kravestky, D.J., Gotlib, V.I., 1990. Highly sensitive thermoluminescent anion-defective α -Al₂O₃:C single crystal detectors. *Radiat. Prot. Dosim.* 32 (1), 15–20.
- Akserlod, M.S., McKeever, S.W.S., Moscovitch, M., Emfietzoglou, D., Durham, J.S., Soares, C.G.A., 1996. Thin-layer Al₂O₃:C beta TL detector. *Radiat. Prot. Dosim.* 66, 105–110.
- Akserlod, M.S., Larsen, N.A., Whitley, V., McKeever, S.W.S., 1998. Thermal quenching of F-centre luminescence in Al₂O₃:C. *J. Lumin.* 131, 1086–1094.
- Bitencourt, J.F.S., Ventieri, K., Gonçalves, K.A., Pires, E.L., Mittani, J.C., Tatum, H.A., 2010. Comparison between neodymium doped alumina samples obtained by Pechini and Sol-gel methods using thermos-stimulated luminescence and SEM. *J. Non-Cryst.* 356 (52–4), 2956–2959.

- Böhm, J., 1986. The National Primary Standard of the PTB for Realizing The Unit Of The Absorbed Dose Rate To Tissue For Beta radiation. Physikalisch-Technische Bundesanstalt, Braunschweig, Germany (PTB-Dos-13: 1986).
- BSS2, 2005. Beta Secondary Standard 2. Operation manual. Isotrak. QSA Global GmbH.
- Caldas, L.V.E., 1986. Performance characteristics of an extrapolation chamber for beta radiation detection. *Appl. Radiat. Isot.* 37 (9), 988–990.
- Cross, W.G., 1997. Empirical expressions for beta ray point source dose distributions. *Radiat. Prot. Dosim.* 69, 85–96.
- DTU Nutech, 2015. Guide to “The Riso TL/OSL Reader”. DTU Nutech, Denmark.
- Ferreira, H.R., Santos, A., 2014. Preparation and characterisation of a SOL-GEL α - Al_2O_3 polycrystalline detector. *Radiat. Prot. Dosim.* 163 (2), 1–7.
- Furetta, C., 2008. Questions and Answers on Thermoluminescence (TL) and Optically Stimulated Luminescence (OSL). World Scientific Publishing, Singapore.
- Furetta, C., Weng, P., 1998. Operational Thermoluminescence Dosimetry. World Scientific Publishing, Singapore.
- Göksu, H.Y., Bulur, E., Wahl, W., 1999. Beta dosimetry using thin-layer α - Al_2O_3 :C TL detectors. *Radiat. Prot. Dosim.* 84 (1–4), 451–455.
- INTERNATIONAL COMMISSION ON RADIATION UNITS AND MEASUREMENTS, 1997. Dosimetry of external beta rays for radiation protection. Bethesda: ICRU, (ICRU Report 56).
- Kalita, J.M., Chithambo, M.L., 2017. Comprehensive kinetic analysis of thermoluminescence peaks of α -. *J. Lumin.* 185, 72–82.
- Kitis, G., 2002. Confirmation of the influence of thermal quenching on the initial rise method in α - Al_2O_3 :C. *Phys. Stat. Sol. (a)* 191 (2), 621–627.
- Kumar, M., Rakesh, R.B., Sneha, C., Ratna, P., Bakshi, A.K., Datta, D., 2016. Beta response of CaSO_4 :Dy based thermoluminescent dosimeter badge and its angular dependence studies for personnel monitoring applications. *Radiat. Prot. Environ.* 39, 132–137.
- Kumar, M., Dhabekar, B., Menon, S., Bakshi, S., Udhayakumar, J., Chougankar, M., Mayya, Y. P., 2013. Beta response of LiMgPO_4 :tb,b based OSL discs for personnel monitoring applications. *Radiat. Prot. Dosim.* 155 (4), 410–417.
- Mancosu, P., Ripamonti, D., Veronese, I., Cantone, M.C., Giussani, A., Tosi, G., 2005. Angular dependence of the TL reading of thin α - Al_2O_3 :C dosimeters exposed to different beta spectra. *Radiat. Prot. Dosim.* 113, 359–365.
- McKeever, S.W.S., Moscovitch, M., 2003. On the advantages and disadvantages of optically stimulated luminescence dosimetry and thermoluminescence dosimetry. *Radiat. Prot. Dosim.* 104, 263–270.
- McKeever, S.W.S., Moscovitch, M., Townsend, P.D., 1995. Thermoluminescence Dosimetry Materials: Properties and uses. Nuclear Technology Publishing, Ashford.
- Nascimento, L.F., Saldarriaga, C.V., Vanhavere, F., D’Agostino, E., Defraene, G., De Deene, Y., 2013. Characterization of OSL Al_2O_3 :C droplets for medical dosimetry. *Radiat. Meas.* 56, 200–204.
- Pagonis, V., Chen, R., Maddrey, J.W., Sapp, B., 2011. Simulations of time-resolved photoluminescence experiments in α - Al_2O_3 :C. *J. Lumin.* 131, 1086–1094.
- Pierre, A.C., 1998. Introduction to Sol-Gel Processing. Kluwer Academic Publishers, New York.
- Pinto, T.N.O., Cecatti, S.G.P., Gronchi, C.G., Caldas, L.V.E., 2008. Application of the OSL technique for beta dosimetry. *Radiat. Meas.* 43, 332–334.
- QE65 Pro, 2018. Ocean Optics QE65 Pro Data Sheet. <http://www.OceanOptics.com>. (Accessed in 10/2018).
- Rivera, T., 2011. Advances in ceramics - synthesis and characterization, processing and specific applications. *Synthesis and Thermoluminescent Characterization of Ceramics Materials*. . <<https://www.intechopen.com/books>>.
- Rodriguez, M.G., Denis, G., Akselrod, M.S., Underwood, T.H., Yukihara, E.G., 2011. Thermoluminescence, optically stimulated luminescence and radioluminescence properties of Al_2O_3 :C,Mg. *Radiat. Meas.* 46 (12), 1469–1473.
- Rotman, S.R., Warde, C., Tuller, H.L., Haggerty, J., 1989. Defect-property correlations in garnet crystals. V. Energy transfer in luminescent yttrium aluminum–yttrium iron garnet solid solutions. *J. Appl. Phys.* 66 (7), 3207–3210.
- Tatumi, S.H., Ventieri, A., Bitencourt, J.F.S., Gonçalves, K.A., Mittani, J.C.R., Rojas, R.R., do Valle S.C., 2012. Effects of heat treatments on the thermoluminescence and optically stimulated luminescence of nanostructured aluminate doped with rare-earth and semi-metal chemical element. Heat Treatment – Conventional and Novel Applications. Open access peer-reviewed edited volume. <<https://www.intechopen.com/books/heat-treatment-conventional-and-novel-applications>>.
- Valle, J.F., Garcia-Guinea, F., Correcher, J.V., 2004. Espectros de emisión de radioluminiscencia y termoluminiscencia de una leucita de Monte Somma (Italia). *Bol. Soc. Esp. Ceram.* 43 (6), 919–924.
- Varney, C.R., Reda, S.M., Mackay, D.T., Rowe, M.C., Selim, F.A., 2011. Strong visible and near infrared luminescence in undoped YAG single crystals. *AIP Adv.* 1, 042170.
- Villani, D., Barbosa, S.A., Campos, L.L., 2017. Caracterização de dosímetros de Al_2O_3 :C para dosimetria de fótons utilizando a técnica OSL. *Braz. J. Radiat. Sci.* 5 (3), 1–13.
- Yukihara, E.G., McKeever, S.W.S., 2008. Optically stimulated luminescence (OSL) dosimetry in medicine. *Phys. Med. Biol.* 53, 351–379.
- Yukihara, E.G., McKeever, S.W.S., 2011. *Optically Stimulated Luminescence: Fundamentals and Applications*. John Wiley & Sons, Singapore.
- Yukihara, E.G., Whitley, V.H., Polf, J.C., Klein, D.M., McKeever, S.W.S., Akselrod, A.E., Akselrod, M.S., 2003. The effects of deep trap population on the thermoluminescence of Al_2O_3 :C. *Radiat. Meas.* 37 (6), 627–638.